

THE EFFECT OF A DISCONTINUITY IN WALL BLOWING ON THE TURBULENT INCOMPRESSIBLE BOUNDARY LAYER

ROGER L. SIMPSON*

Department of Mechanical Engineering, Stanford University, Stanford, California, U.S.A.

(Received 11 August 1970 and in revised form 2 February 1971)

Abstract—Experiments are reported for two-dimensional incompressible turbulent boundary layers for which there was an abrupt change in wall blowing. Skin-friction and mean velocity profile results indicate that asymptotically downstream the flow behaves according to the local momentum thickness Reynolds number and blowing conditions. It is found that during the relaxation length, the flow is separated by a ‘penetration point’ trajectory into an outer region described by upstream conditions and an inner region dependent upon local blowing conditions. The path of these trajectories appear very independent of the downstream wall condition.

The penetration point trajectories are found to closely coincide with the last upstream outgoing characteristic of the hyperbolic set of governing partial differential equations presented by Bradshaw, Ferriss and Atwell [4]. These results suggest that the outgoing characteristic is more than a mathematical result and can be observed experimentally with flows with abrupt changes in wall blowing.

NOMENCLATURE

$C_f/2$,	friction factor defined by	V ,	mean velocity perpendicular to the wall [ft/s];
H ,	$\tau_w \equiv (C_f/2)\rho_\infty U_\infty^2$; $\equiv \delta^*/\theta$, profile shape parameter;	V_w^+ ,	$= V_w/U_\tau$;
P ,	pressure [lbf/ft ²];	v ,	fluctuation velocity perpendicular to the wall [ft/s];
p ,	pressure fluctuation [lbf/ft ²]; also denotes a point in space;	w ,	transverse velocity fluctuation [ft/s];
$\overline{q^2}/2$,	$= (\overline{u^2} + \overline{v^2} + \overline{w^2})/2$, turbulence energy per unit mass [lbf-ft/lbm];	x ,	distance along the plate [ft];
Re ,	Reynolds number based on the momentum thickness θ or X position;	y ,	distance perpendicular to the plate [ft];
U ,	mean velocity in the main-stream direction [ft/s];	y^+ ,	yU_τ/v ;
U^+ ,	$= U/U_\tau$;	γ ,	dummy variable;
U_τ ,	$\equiv \sqrt{\tau_w/\rho}$, shear velocity [ft/s];	δ ,	$\equiv y$ at $U/U_\infty = 0.990$, boundary layer thickness [ft];
u ,	main-stream direction velocity fluctuation [ft/s];	δ^* ,	$\equiv \int_0^\infty \left(1 - \frac{\rho U}{\rho_\infty U_\infty}\right) dy$, displacement thickness [ft];
		v ,	kinematic viscosity [ft ² /s];
		ξ ,	x position of a step change in V_w [ft];
		ρ ,	density [lbm/ft ³];
		τ ,	shear stress [lbf/ft ²].

* At present at Thermal and Fluid Sciences Center, Institute of Technology, Southern Methodist University, Dallas, Texas, 75222.

Subscripts

- max, maximum value;
 p , denotes penetration point;
 w , wall condition;
 ∞ , free-stream condition.

INTRODUCTION

THE RESPONSE of a turbulent boundary layer to a strong perturbation from its equilibrium state has been given increasing attention in recent years. The response of a turbulent boundary layer to abrupt changes in surface roughness is of practical importance in meteorology (Taylor [1]). Future atmospheric re-entry vehicles may employ permeable surfaces for transpiration cooling that are separated by solid surfaces for structural integrity. Hence, the turbulent boundary layer flowing over this alternately blowing-no blowing surface is strongly perturbed from its equilibrium state. In addition, the search for a better understanding of the structure of turbulent flows has motivated the study of flows with sudden changes of free-stream pressure gradient or wall conditions and flows perturbed by obstacles (Tani [2]).

The present work reports experiments on constant free-stream velocity, incompressible, turbulent boundary layers subjected to a sudden increase in the wall blowing rate.

These experiments and the experiment of Levitch [3] for an abrupt decrease in wall blowing are shown to support the hyperbolic character of the time-averaged turbulent boundary layer as reported by Bradshaw *et al.* [4], thus adding some understanding of the structure of turbulent flows.

THE EXPERIMENTAL APPARATUS

The Stanford Heat and Mass Transfer Apparatus, as described in detail by Moffat and Kays [5] was used in the experiments of Simpson [6]. The stagnation pressure probe instrumentation and fluid dynamic characteristics of the apparatus are discussed in detail by Simpson [6] and Simpson *et al.* [7]. As a result of qualification tests, the boundary layer flow

was found to be essentially steady, two-dimensional, constant property, constant free-stream velocity turbulent flow over a smooth uniformly permeable flat plate. Simpson and Whitten [8] calibrated Preston tubes with transpiration on this apparatus. Heat transfer and temperature profile data from this apparatus are reported by Moffat and Kays [5] and Whitten [9]. Simpson *et al.* [10] used data from this apparatus to determine the effect of transpiration on the turbulent Prandtl number distribution in the boundary layer. The unblown flat plate skin friction and heat transfer coefficient results agreed with accepted correlations while the mean velocity profiles were found to be "normal" according to the criterion proposed by Coles [11].

EXPERIMENTAL SKIN FRICTION RESULTS

The skin friction results from this apparatus for a constant free-stream velocity flow with uniform or slowly varying wall blowing have been discussed in considerable detail elsewhere (Simpson, [6] and Simpson *et al.* [7]). Two methods were used in determining these friction factors. One method used the momentum integral equation, differentiating a smooth fit of

$$Re_{\theta} - \int_0^{Re_x} (\rho_w V_w / \rho_{\infty} U_{\infty}) d(Re_y) \text{ vs. } Re_x,$$

experimentally determined along the flow duct for each run. The second method used the viscous sublayer velocity profile equation relating experimental velocity points in the viscous sublayer to $C_f/2$ in terms of the mass flux $(\rho V)_w$ and $(\rho U)_{\infty}$. With exception of two out of 95 velocity profile traverses, the values of $C_f/2$ for a given traverse obtained by both methods agreed within the uncertainty estimated at 20:1 odds. The heat transfer analogue ($St \approx 1.16C_f/2$) provided supporting evidence for the results reported by Simpson *et al.* [7].

Downstream of a step change in the wall blowing condition, a fit of

$$Re_\theta - \int_0^{Re_x} (\rho_w V_w / \rho_\infty U_\infty) d(Re_x) \text{ vs. } Re_x$$

showed much curvature, making $C_f/2$ values obtained by differentiating this fit highly uncertain. Hence, only the viscous sublayer method was used to obtain $C_f/2$ downstream of an abrupt increase in wall blowing. Presumably,

the flow near the wall in the viscous sublayer reacts to local wall conditions rapidly, with the relaxation length of the order of several sublayer thicknesses. Therefore, the sublayer method should be valid downstream of this relaxation length since the results from this technique were in close agreement with momentum integral equation results for uniform blowing and suction cases at closely the same unit Reynolds numbers.

The $C_f/2$ results for abrupt changes in blowing are presented in Table 1 with associated

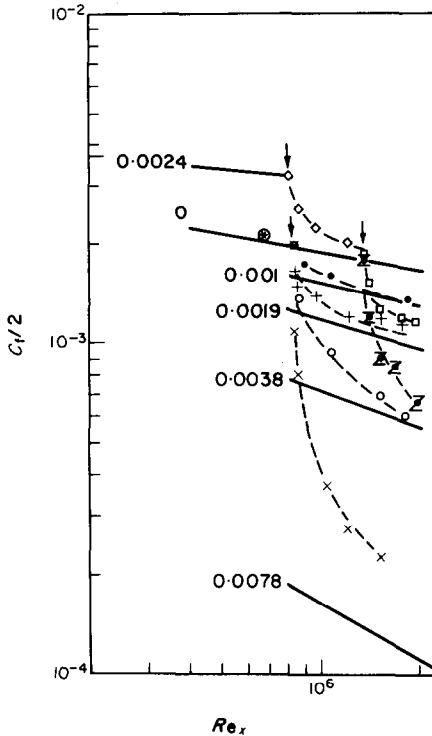


FIG. 1. Sublayer method $C_f/2$ vs. Re_x for step changes in V_w .

Solid lines denote uniform V_w/U_∞ data [7]; dashed lines visual aids only; arrows denote position of step change.

$Re_x \times 10^{-5}$	Re_θ at step	V_w/U_∞ upstream of change	V_w/U_∞ downstream of change
◇ 7.95	906	-0.0024	0.0000
● 8.14	1944	0.0000	0.0010
+ 8.06	1957	0.0000	0.0020
□ 13.4	3023	0.0000	0.0020
○ 8.15	1967	0.0000	0.0039
■ 13.3	3021	0.0000	0.0040
× 8.10	2019	0.0000	0.0080

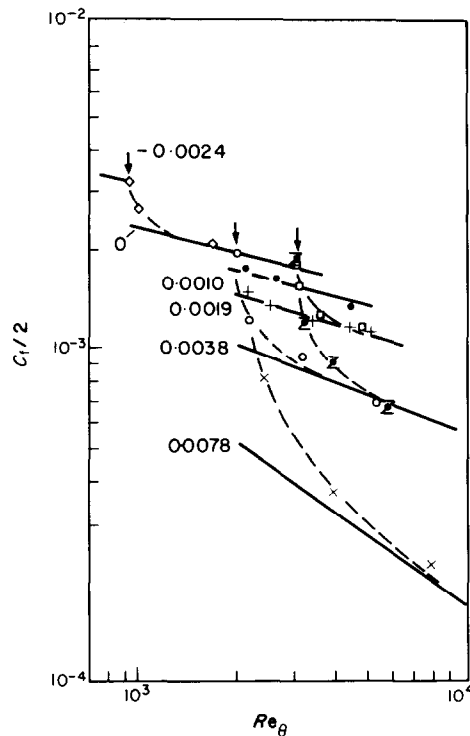


FIG. 2. Sublayer method $C_f/2$ vs. Re_θ for step changes in V_w .

uncertainty estimates for seven isothermal constant free-stream velocity flows obtained under the test conditions:

- X—Reynolds number $6.75 \times 10^5 - 2 \times 10^6$
- Blowing fraction, V_w/U_∞ -0.0024 to 0.0080
- Free-stream velocity, fps 42-44
- Free-stream temperature, °F 65-71

Table 1. Experimental data for flows with abrupt changes in wall blowing

Position of date/step, $Re_x \times 10^{-5}$	$V_w/U_\infty \times 10^{-3}$	$Re_x \times 10^{-5}$	$(Re_x - Re_x) \times 10^{-4}$	Re_θ	H	$C_f/2 \times 10^3$	Penetration point U_p/U_∞
62367/7-95	± 0.66	$\pm 0.25\%$	$\pm 3\%$	$\pm 2\%$	± 0.04	± 0.2	± 0.05
$M = 1$	-2.399	7.90		906	1.312	3.22	0.00
$M = 2$	0.000	8.56	5.98	989	1.348	2.58	0.87
	0.000	9.50	15.3			2.26	
$M = 3$	0.000	11.9	39.6	1722	1.389	2.00	1.00
42567/8-14	± 0.1	$\pm 0.25\%$	$\pm 3\%$	$\pm 1\%$	± 0.03	± 0.2	± 0.05
$M = 1$	0.000	6.75		1676	1.386	2.10	0.00
$M = 2$	0.000	8.11		1944	1.383	2.05	0.00
$M = 3$	1.025	8.58	4.36	2065	1.394	1.73	0.75
$M = 4$	1.024	10.4	22.5	2590	1.420	1.62	0.95
$M = 5$	1.017	17.7	95.0	4399	1.415	1.39	1.00
42767/8-06	± 0.07	$\pm 0.25\%$	$\pm 3\%$	$\pm 1\%$	± 0.03	± 0.2	± 0.05
	0.000	6.70				2.11	
$M = 1$	0.000	8.03		1957	1.382	2.06	0.00
	2.018	8.23	1.6			1.66	
$M = 2$	2.018	8.47	4.0	2110	1.412	1.51	0.78
$M = 3$	1.995	9.67	15.7	2497	1.450	1.38	0.87
$M = 4$	1.960	12.1	40.0	3285	1.475	1.21	0.95
$M = 5$	1.969	15.1	69.9	4346	1.476	1.20	1.00
$M = 6$	1.958	17.6	94.5	5015	1.473	1.15	1.00
5167/8-15	± 0.064	$\pm 0.25\%$	$\pm 3\%$	$\pm 1\%$	± 0.03	± 0.2	± 0.05
	0.000	6.76				2.11	
$M = 1$	0.000	8.09		1967	1.384	1.95	0.00
	3.917	8.35	1.9			1.38	
$M = 2$	3.917	8.55	3.96	2133	1.441	1.23	0.78
$M = 3$	3.885	10.4	22.5	3135	1.561	0.95	0.97
$M = 4$	3.939	14.9	67.4	5283	1.618	0.70	1.00
	3.939	17.6	94.7			0.61	
5267/8-10	± 0.063	$\pm 0.25\%$	$\pm 3\%$	$\pm 1\%$	± 0.02	± 0.3	± 0.05
	0.000	6.72				2.11	
$M = 1$	0.000	8.04		2019	1.384	1.95	0.00
	7.981	8.25	1.5			1.10	
$M = 2$	7.981	8.53	3.9	2355	1.530	0.81	0.77
$M = 3$	7.944	10.4	22.5	3842	1.871	0.37	0.95
	7.966	12.2	40.5			0.28	
$M = 4$	7.988	15.1	69.5	7755	2.005	0.23	1.00
5467/13-4	± 0.07	$\pm 0.25\%$	$\pm 3\%$	$\pm 1\%$	± 0.03	± 0.2	± 0.05
$M = 1$	0.000	13.3		3023	1.365	1.86	0.00
$M = 2$	2.004	13.6	1.7	3040	1.376	1.52	0.47
	2.004	13.85	3.97			1.48	
$M = 3$	2.010	14.9	15.4	3543	1.427	1.27	0.85
	2.015	17.3	40.0			1.22	
$M = 4$	2.018	19.1	57.3	4778	1.461	1.17	1.00
5867/13-3	± 0.064	$\pm 0.25\%$	$\pm 3\%$	$\pm 1\%$	± 0.03	± 0.2	± 0.05
$M = 1$	0.000	13.2		3021	1.369	1.80	0.00
$M = 2$	4.043	13.6	4.03	3144	1.417	1.20	0.73
$M = 3$	3.999	14.8	15.3	3821	1.504	0.90	0.87
	4.000	16.4	30.8			0.85	
$M = 4$	4.008	19.0	57.0	5637	1.615	0.66	1.00

In addition to the 27 complete velocity traverses, for which Re_θ and H are reported, 11 partial traverses near the wall were made to determine $C_f/2$. The X -Reynolds number at the abrupt change in blowing, Re_ξ , was either 8×10^5 or 1.3×10^6 . The Reynolds numbers from the abrupt change, $Re_x - Re_\xi$, are also reported.

These $C_f/2$ results are shown on Fig. 1 as a function of Re_x . At the step change, the $C_f/2$ decreases from the upstream $C_f/2$, asymptotically approaching at high Re_x the slope of the results obtained had there been the same blow-

ing or suction condition from the origin of the boundary layer. The same $C_f/2$ results when plotted in Fig. 2 vs. Re_θ indicate that asymptotically downstream, $C_f/2$ is determined by the local Re_θ and blowing condition.

INTERPRETATION OF EXPERIMENTAL VELOCITY PROFILE RESULTS

For interpretation of the effect of an abrupt change in wall blowing on the velocity profile, we will consider the data of Levitch [3] in addition to the data of Simpson [6]. Levitch

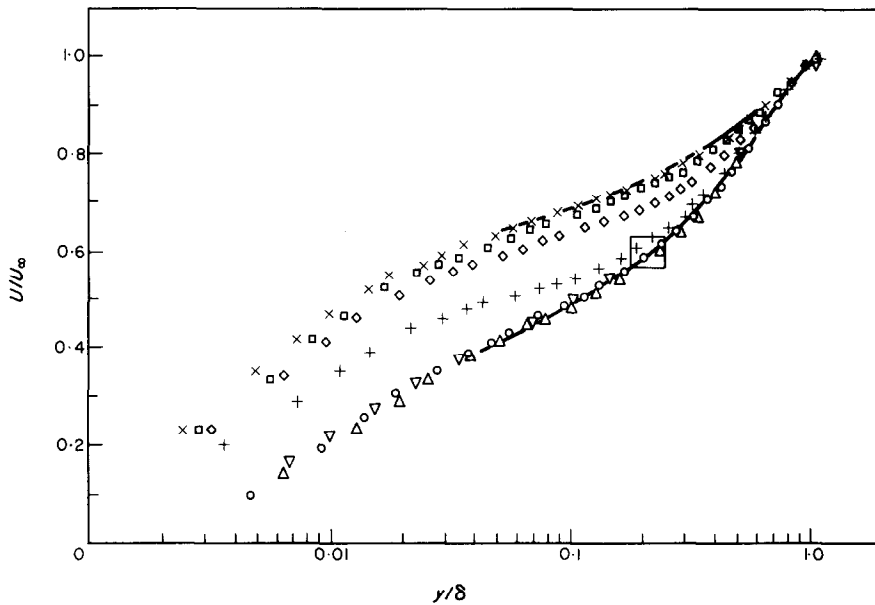


FIG. 3. Velocity profile data of Levitch [3] for an abrupt decrease in wall blowing. Solid line denotes $V_w/U_\infty = 0.0045$ constant V_w data; dashed line denotes $V_w/U_\infty = 0.000$ constant V_w data; large box denotes penetration point region for the station E profile.

Station	V_w/U_∞	Re_θ	$C_f/2 \times 10^3$	$\tau_{max}/\rho U_\infty^2 \times 10^3$
Δ C	0.0045	2915	0.75	
\circ D	0.0045	4060	0.65	3.02
+	0.000	4975		
\diamond F	0.000	5200		
\square G	0.000	5540		
\times H	0.000	5945		
∇ Simpson (1967)	0.0045	4145	0.66	3.04

made measurements on a 25 fps constant free-stream velocity incompressible turbulent boundary layer. For the first 83 in. of test wall there was blowing, $V_w/U_\infty = 0.0045$. The blowing was then discontinued. The flow in the test section was reported to have exhibited some three-dimensional effects. However, measurements were not made at the center plane, but half way to the side wall, presumably where the flow was considered unaffected by the three-dimensionality.

Simpson [6, 12] observed that for zero injection or uniform injection or suction on a two-dimensional flow, there is U/U_∞ vs. y/δ similarity independent of Re_θ in the region outside the sublayer for $1000 < Re_\theta < 6000$. Figure 3 shows that upstream of the discontinuity in injection, Levitch's data obeys this similarity and is in close agreement with a profile of Simpson [6] for the same blowing rate and closely the same Re_θ . Far downstream of the discontinuity in blowing we see that Levitch's profiles approach

the unblown velocity profile similarity shown by Simpson's unblown data. Hence, Levitch's profiles are not noticeably affected by any three-dimensionality of the flow.

Figures 3-6 illustrate velocity profiles from typical step change runs plotted as U/U_∞ vs. y/δ . Just upstream of the step, the flow and entire velocity profile are determined by the upstream blowing or sucking condition. As the flow passes the step change, the velocity profile near the wall changes rapidly while the velocity profile near the freestream continues to behave according to the upstream wall condition. That point (or locality) of a profile which separates these two regions is referred to as the *penetration point*.

Figure 7 presents the penetration point velocity, U_p/U_∞ , versus the distance downstream of the step, $Re_x - Re_\xi$ for the data of Simpson and Levitch. One would expect that possibly $Re_x - Re_\xi$, Re_θ at the step, V_w/U_∞ upstream, V_w/U_∞ downstream, and the character of the

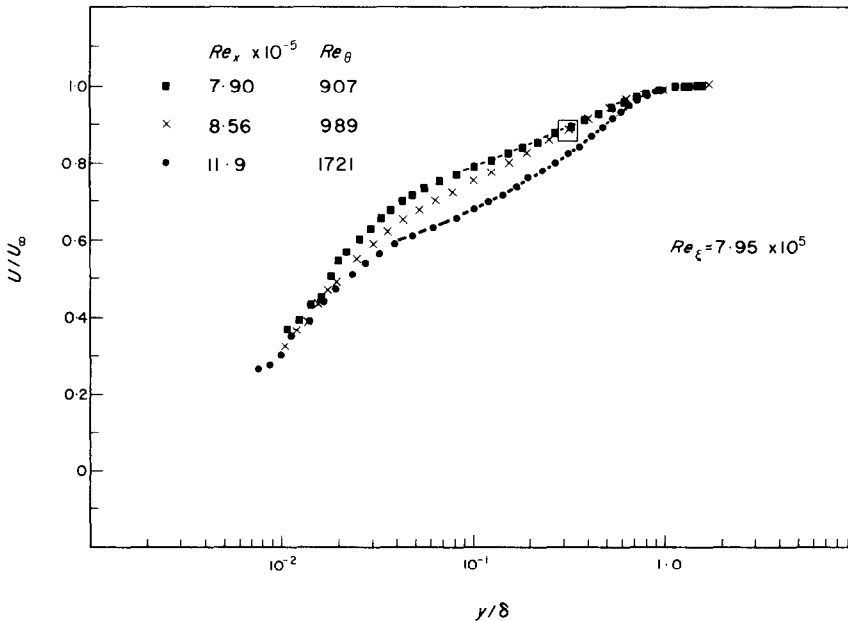


FIG.4. Velocity profile data for a sucked-unsucked step change, 62367 run. Dashed line denotes $V_w/U_\infty = 0.000$ constant V_w data; large box denotes penetration point region for second profile.

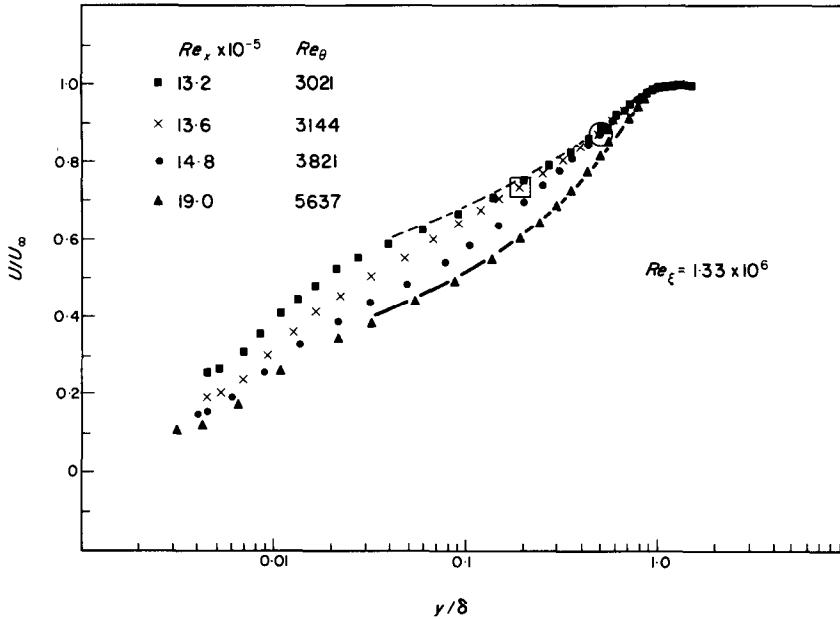


FIG. 5. Velocity profile data for an unblown-blown step change, 5867 run; $V_w/U_\infty = 0.004$ downstream. Dashed line denotes $V_w/U_\infty = 0.00$ constant blowing data; solid line denotes $V_w/U_\infty = 0.0038$ constant blowing data; large box and circle denote penetration point regions for second and third profiles, respectively.

test wall could affect how U_p/U_∞ behaved. For the data of Simpson where the same upstream boundary layer was subjected to different step increases in blowing, no effect of the downstream V_w/U_∞ on the penetration point U_p/U_∞ was detected. Only two values of the Re_θ at the step increase were examined by Simpson, $Re_\theta = 2000$ and $Re_\theta = 3000$. Keeping in mind that a wide range of Re_θ values at the step was not investigated by Simpson, no strong effect of Re_θ at the step was found on U_p/U_∞ . Because of the different upstream blowing or suction conditions, the penetration point U_p/U_∞ vs. $Re_x - Re_\xi$ relationship appears to be different for the cases of upstream suction, no suction or blowing upstream, and upstream blowing. The downstream flow does not appear to influence the U_p/U_∞ vs. $Re_x - Re_\xi$ relationship.

For the cases of uniform or slowly varying

blowing or suction, Simpson [6, 12] found that

$$U^+ = \frac{1}{V_w^+} [\exp(V_w^+ y^+) - 1] \quad (1)$$

described the velocity profile in the viscous sublayer while

$$\begin{aligned} \phi &= \frac{2}{V_w^+} [(1 + U^+ V_w^+)^{\frac{1}{2}} - (1 + 11V_w^+)^{\frac{1}{2}}] \\ &= \frac{1}{0.44} \ln \left| \frac{y^+}{11} \right| \end{aligned} \quad (2)$$

was found to fit the fully turbulent wall region velocity profile data.* One would expect that

* The Kármán constant value of 0.44 is the result of averaging the low Reynolds number effect ($Re_\theta < 6000$) over the range of experimental data. A detailed description of this low Reynolds number effect is given by Simpson [12].

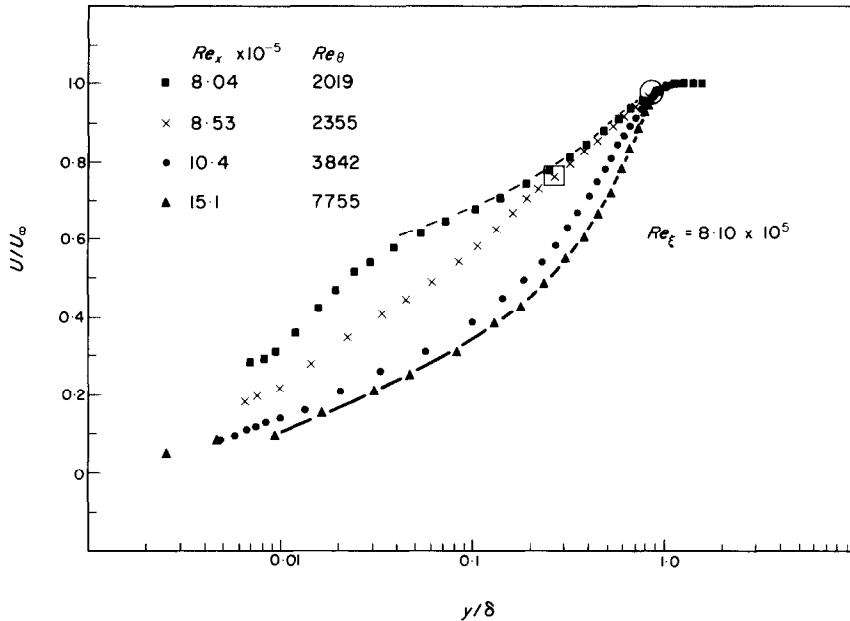


FIG. 6. Velocity profile data for an unblown blown step change, 5267; $V_w/U_\infty = 0.00$ upstream, $V_w/U_x = 0.008$ downstream. Dashed line denotes $V_w/U_\infty = 0.00$ constant blowing data; solid line denotes $V_w/U_\infty = 0.0078$ constant blowing data; large box and circle denote penetration point regions for second and third profiles, respectively.

the region nearer the wall ($U/U_\infty < U_p/U_\infty$) could be described by local downstream wall conditions. It was found that indeed for $U/U_\infty < U_p/U_\infty$

$$U^+ = f(y^+, V_w^+) \quad (3)$$

based on local downstream conditions was satisfied. Equation (1) naturally satisfies the viscous sublayer data downstream of the sublayer relaxation zone, since the viscous sublayer method was used by Simpson to get $C_f/2$. Figures 8 and 9 are typical ϕ vs. y^+ plots which demonstrate the validity of equation (2) for the fully turbulent region where $U/U_\infty < U_p/U_\infty$.^{*} The outer region ($U/U_\infty > U_p/U_\infty$) should be described by what the profile would have been had the upstream condition prevailed downstream. This latter statement was found true and can be observed in Figs. 3–6.

Figure 10 summarizes the flow model deduced from the experimental results. Flow region A is described by upstream conditions while region

^{*} Levitch used his assumed law-of-the-wall with blowing in a Preston tube technique to determine $C_f/2$. He found his $C_f/2$ results in agreement with those of Mickley and Davis, apparently justifying his method. However, Rotta, Stevenson and Kinney (Simpson *et al.* [7]) each corrected the Mickley-Davis data for the small imposed pressure gradient, producing much higher $C_f/2$ values than obtained by Mickley and Davis. These higher $C_f/2$ values for uniform blowing were found (Simpson *et al.* [7]) in good agreement with the uniform blowing data of Simpson [6]. For this reason, new $C_f/2$ results for Levitch's blown profiles were obtained by fitting equation (2) to his profiles, yielding the results presented beneath Fig. 3. Note that for the same blowing rate and nearly the same Re_θ , the $C_f/2$ results for a profile of Levitch and a profile of Simpson are in close agreement. Furthermore note that for these same profiles, $\tau_{\max}/\rho_\infty U_\infty^2$ obtained by Levitch by hot-wire measurements are in close agreement with the results of Simpson, giving more support to the recalculated $C_f/2$ for Levitch's data. Hence, the recalculated $C_f/2$ values are used in the theoretical considerations below.

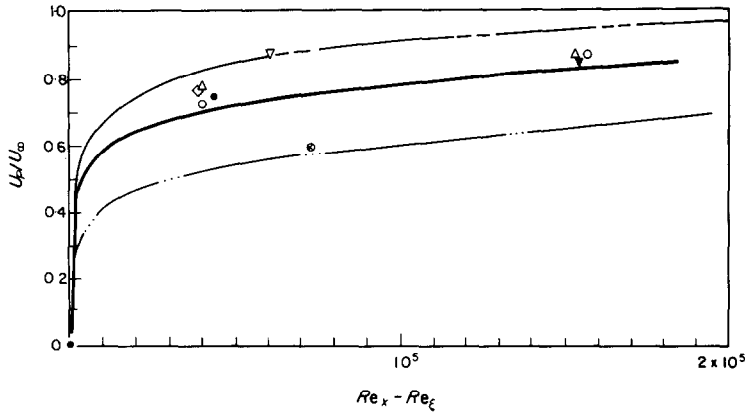


FIG. 7. Penetration point velocity, U_p/U_∞ vs. $Re_x - Re_z$. Prediction from equation (8): dashed line— $V_w/U_\infty = -0.0024$ upstream; solid line— $V_w/U_\infty = 0.00$ upstream; dotted line— $V_w/U_\infty = 0.0045$ upstream. Experimental uncertainty: 0.05 in U_p/U_∞ ; 3 per cent in $Re_x - Re_z$.

$Re_z \times 10^{-5}$	V_w/U_∞ upstream of change	V_w/U_∞ downstream of change
▽ 7.95	-0.0024	0.0000
● 8.14	0.000	0.0010
△ 8.06	0.000	0.0020
□ 8.15	0.000	0.0039
◇ 8.10	0.000	0.0080
▼ 13.4	0.000	0.0020
○ 13.3	0.000	0.0040
⊗ 10.4	0.0045	0.000 Levitch

B is described by the local wall conditions. The behavior of the penetration point trajectory separating these two regions is strongly independent of downstream conditions but is dependent upon the properties of the oncoming boundary layer at the step change. Were one able to predict the behavior of U_p/U_∞ , one would be able to predict the boundary layer behavior downstream of the step change. The theoretical considerations to be described next, closely predict the behavior of the penetration point trajectory.

boundary-layer momentum, and turbulence energy equations for two dimensions

$$\frac{\partial U}{\partial x} + \frac{\partial V}{\partial y} = 0 \tag{4}$$

$$U \frac{\partial U}{\partial x} + V \frac{\partial U}{\partial y} = -\frac{1}{\rho} \frac{dP}{dx} + \frac{1}{\rho} \frac{\partial \tau}{\partial y} \tag{5}$$

$$\frac{1}{2} \rho \left(\underbrace{U \frac{\partial \overline{q^2}}{\partial x}}_{\text{advection}} + \underbrace{V \frac{\partial \overline{q^2}}{\partial y}}_{\text{advection}} \right) - \underbrace{\frac{\tau \partial U}{\partial y}}_{\text{production}} + \underbrace{\frac{\partial}{\partial y} (\overline{pv} + \frac{1}{2} \rho \overline{q^2 v})}_{\text{diffusion}} + \underbrace{\rho \epsilon}_{\text{dissipation}} = 0 \tag{6}$$

THEORETICAL CONSIDERATIONS*

The incompressible time averaged continuity,

* This work followed the Stanford experiments by two years, therefore not influencing the preceding interpretation of the experimental results.

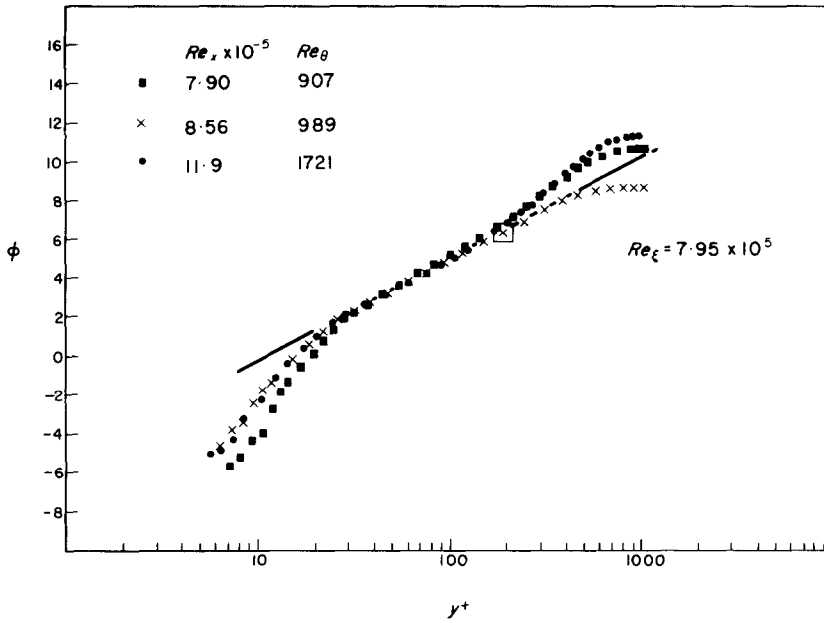


FIG. 8. Law of the wall downstream of a sucked-unsucked step change, 62367 run; $V_w/U_\infty = 0.0024$ upstream, $V_w/U_\infty = 0.00$ downstream. Solid line denotes equation (2). Large box denotes penetration point region for second profile.

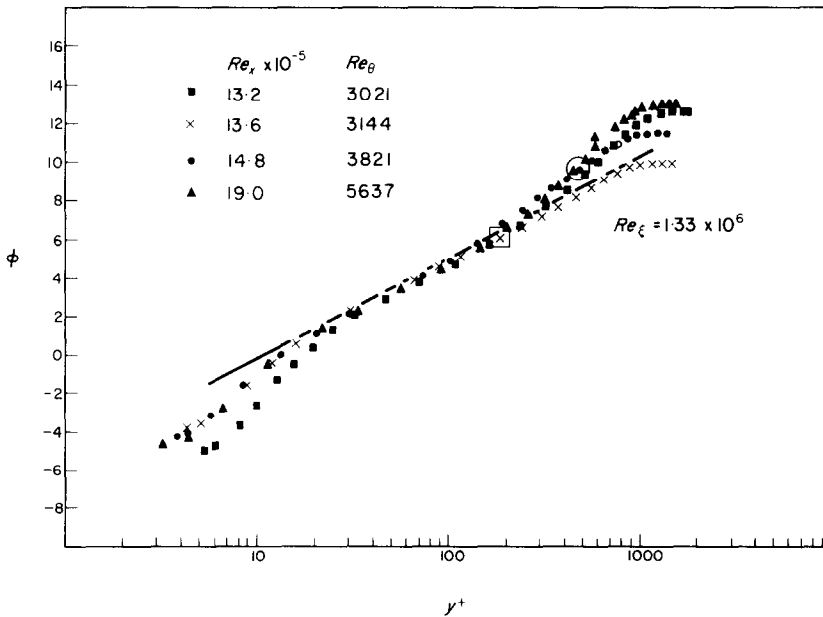


FIG. 9. Law of the wall downstream of an unblown-blown step change, 5867 run; $V_w/U_\infty = 0.000$ upstream, $V_w/U_\infty = 0.004$ downstream. Solid line represents equation (2). Large box and circle denote penetration point regions for second and third profiles, respectively.

form a hyperbolic set of equations if the energy diffusion is produced by large eddy motions. Bradshaw, Ferriss and Atwell [4], with the aid

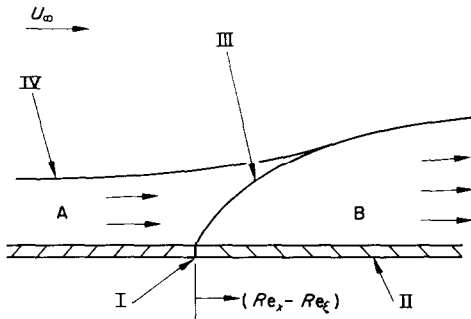


FIG. 10. Flow model for abrupt changes in blowing or suction at the wall. Legend; I—position of a step change in blowing or sucking; II—permeable wall; III—trajectory of penetration point, also last outgoing characteristic of the upstream region; IV—trajectory of boundary layer thickness.

of Mr. P. G. Williams of NPL, pointed this out. If a “gradient diffusion” form is used to represent the energy diffusion, a term $\partial^2 \tau / \partial y^2$ appears and the equations become parabolic. The large eddy motion diffusion appears more reasonable because of the physical interpretation given to the hyperbolic set. Further evidence is given by the fact that Simpson, Whitten and Moffat [10] have shown that the large eddy motion diffusion concept successfully predicts the turbulent Prandtl number distribution for a turbulent boundary layer.

As pointed out by Bradshaw *et al.* [4], there are three real characteristic directions associated

with these three equations, along which the partial differential equations reduce to ordinary differential equations containing gradients along the characteristics only. For this three equation set of interest, the three characteristics are given by

$$\frac{dy}{dx} = \tan \alpha = \infty,$$

$$\left\{ V + \frac{\overline{pv} + \frac{1}{2}\overline{\rho q^2 v}}{\overline{\rho q^2}} \pm \left[\left(\frac{\overline{pv} + \frac{\overline{\rho q^2 v}}{2}}{\overline{\rho q^2}} \right)^2 + \frac{2\tau}{\overline{\rho q^2}} \left(\frac{\tau}{\rho} \right) \right]^{\frac{1}{2}} \right\} / U. \quad (7)$$

In other words, one characteristic direction is normal to the test wall, while another is inclined further from the wall than the mean streamline (outgoing characteristic) and the third is inclined closer to the wall than the mean streamline (incoming characteristic). The physical significance of the hyperbolicity is that the effect of a small disturbance at some point p in a turbulent boundary layer is restricted to the downstream side of the characteristics passing through p .

We can attach possible further physical significance to the outgoing characteristics: *for abrupt changes in the wall boundary condition, the apparent penetration point trajectory coincides with the last outgoing characteristic described by the upstream boundary layer.* The fact that we experimentally found no effect of the downstream wall condition on the penetration point trajectory supports this idea. To verify this idea we can integrate the equation for the outgoing characteristic

$$x - \xi = \int_{y=0}^y \frac{U dy}{V + \frac{\overline{pv} + \frac{1}{2}\overline{\rho q^2 v}}{\overline{\rho q^2}} + \left\{ \left(\frac{\overline{pv} + \frac{1}{2}\overline{\rho q^2 v}}{\overline{\rho q^2}} \right)^2 + \frac{2\tau}{\overline{\rho q^2}} \left[\frac{\tau}{\rho} \right] \right\}^{\frac{1}{2}}} \quad (8)$$

to obtain the y vs. $x - \xi$ position of an outgoing characteristic beginning on the wall at position ξ^- . We insert into this equation values for the boundary layer immediately upstream: the experimentally determined quantities for U_τ and U/U_∞ , V/U_∞ , and τ/τ_w profiles (tabulated by Simpson [6] and discussed by Simpson [12]) and the turbulence profile correlations of Bradshaw *et al.* [4]. As discussed in the Appendix, these turbulence correlations appear (unfortunately only through plausibility arguments to date) to be independent of blowing and moderate

downstream blowing condition. This downstream location or relaxation length was calculated by equation (8) for each experimental flow of Simpson and Levitch. These results, normalized on the boundary layer thickness at the abrupt change, are presented in Table 2. The experimental relaxation lengths presented in Table 2 were determined by observing the first downstream location where the entire mean velocity profile was apparently given by the local Re_θ and blowing condition. It should be remembered that not many experimental velocity

Table 2. Relaxation lengths downstream of an abrupt change in wall blowing

	V_w/U_∞ upstream	V_w/U_∞ downstream	$(X - \xi)_{\text{relaxation}}/\delta_{\text{step}}$	
			Experimental ± 5	Calculated
Simpson (1967)	0.0024	0.0	≈ 40	50
	0.000	0.001-	$\approx 34-40$	37.2
		0.008		
Levitch (1966)	0.00452	0.0	≈ 25	19.5

suction. Results from this procedure in terms of U_p/U_∞ vs. $Re_x - Re_\xi$ are shown on Fig. 7 for the cases in which experimental data were available. Note the reasonably good agreement between the predicted and experimental values.* Hence the flow model shown on Fig. 10 is completely specified: the penetration point trajectory is given by the upstream quantities in equation (8) while region A is completely described by upstream conditions and region B is described by the penetration point trajectory and the downstream wall conditions.

That position where the penetration point trajectory reaches the outer edge of the boundary layer is the first location where the boundary layer should be completely specified by the

profiles were obtained, making close experimental determination of the relaxation distance difficult. Even so, there is agreement within about 20 per cent for these values, giving more support to equation (8).

DISCUSSION AND CONCLUSIONS

These experimental results indicate that when a turbulent boundary layer undergoes an abrupt change in wall blowing, the boundary layer relaxes asymptotically from the upstream condition to the local downstream blowing condition. Furthermore, it appears that the flow model of Fig. 10 specifies the flow in this relaxation region: a penetration point trajectory separates region A, specified by the upstream wall condition from region B, specified by the downstream wall condition. The "law of the wall with blowing" proposed by Simpson [6, 12] describes the local downstream wall flow in this relaxation region.

* There is a small effect of the value of Re_θ at the abrupt change. There is only about 3 per cent net difference between U_p/U_∞ for a given $Re_x - Re_\xi$ for the $Re_\theta = 2000$ and $Re_\theta = 3000$ runs of Simpson. This is of course much less than the estimated uncertainty of the experimental results.

These experimental results also tend to support the hyperbolic character of the turbulent boundary layer as proposed by Bradshaw *et al.* [4]. The equations of continuity, momentum, and turbulence energy that form this hyperbolic set of equations produce three real characteristics. The penetration point trajectory separating regions A and B was found to closely coincide with the last outgoing characteristic given by the upstream flow. Hence, the outgoing characteristic appears to be more than just a mathematical result: it can be produced experimentally by flows with abrupt changes in wall blowing.

The outgoing characteristic may have more physical significance. For example, Kline *et al.* [13] note that their dye injection studies indicate a "bursting" of turbulent fluid away from the wall. They presented in Fig. 17 of that paper the y vs. x average position of much instantaneous burst data taken for $y^+ < 120$ on a flat plate flow. For those test conditions, equation (8) was used to predict the outgoing characteristic originating from the same position as the dye bursts. The shape of the experimental burst trajectory and the outgoing characteristic are very similar with the x position of the outgoing characteristic being closely 2:1 times the x position of the burst trajectory for the same y position. While there is not close quantitative agreement, the fact that the shape of the two trajectories agree tends to imply some relation yet unknown. Further experiments should be performed to define this possible relation.

ACKNOWLEDGEMENTS

The author thanks the National Science Foundation for financial assistance through a Traineeship while at Stanford University. Appreciation is extended to the Institute of Technology, Southern Methodist University, for computer time for the Theoretical Considerations.

REFERENCES

1. P. A. TAYLOR, On wind and shear stress profiles above a change in surface roughness, *Q. Jl R. Met. Soc.* **95**, 77-91 (1969).
2. I. TANI, Review of some experimental results on the response of a turbulent boundary layer to sudden

perturbations, *Proceedings Computation of Turbulent Boundary Layers—1968 AFOSR-IFP-Stanford Conference*, Vol. I, pp. 483-494 (1968).

3. R. N. LEVITCH, The effect of the discontinuation of injection on the transpired turbulent boundary layer, Sc.D. Thesis, Massachusetts Institute of Technology (1966).
4. P. BRADSHAW, D. H. FERRISS and N. P. ATWELL, Calculation of the boundary layer development using the turbulent energy equation, *J. Fluid Mech.* **28**, part 3, 593-616 (1967).
5. R. J. MOFFAT and W. M. KAYS, The turbulent boundary layer on a porous plate: Experimental heat transfer with uniform blowing and suction, *Int. J. Heat Mass Transfer* **10**, 1547-1566 (1968); also Stanford University Dept. of Mech. Engr. Rep. HMT-1 (1967).
6. R. L. SIMPSON, The turbulent boundary layer on a porous plate: An experimental study of the fluid dynamics with injection and suction, Ph.D. Dissertation, Stanford University (1967).
7. R. L. SIMPSON, R. J. MOFFAT and W. M. KAYS, The turbulent boundary layer on a porous plate: Experimental skin friction with variable injection and suction, *Int. J. Heat Mass Transfer* **12**, 771-791 (1969).
8. R. L. SIMPSON and D. G. WHITTEN, Preston tubes in the transpired turbulent boundary layer, *AIAA Jl* **6**, 1776-1777 (1968).
9. D. G. WHITTEN, The turbulent boundary layer on a porous plate: Experimental heat transfer with variable suction, blowing and surface temperature, Stanford Univ. Dept. of Mech. Engr. Rep. HMT-3 (1967).
10. R. L. SIMPSON, R. J. MOFFAT and D. G. WHITTEN, An experimental study of the turbulent Prandtl number of air injection and suction, *Int. J. Heat Mass Transfer* **13**, 125-143 (1970).
11. D. E. COLES, The turbulent boundary layer in a compressible fluid, RAND Rep. No. R-403-PR (1962).
12. R. L. SIMPSON, Characteristics of turbulent boundary layers at low Reynolds numbers with and without transpiration, *J. Fluid Mech.* **42**, 769-802 (1970).
13. S. J. KLINE, W. C. REYNOLDS, F. A. SCHRAUB and P. W. KUNSTADLER, The structure of turbulent boundary layers, *J. Fluid Mech.* **30**, 741-773 (1967).
14. P. S. KLEBANOFF, Characteristics of turbulence in a boundary layer with zero pressure gradient, NACA TN 3178 (1954).
15. P. BRADSHAW, The turbulence structure of equilibrium boundary layers, *J. Fluid Mech.* **29**, part 4, 625-645 (1967).

APPENDIX

In order to calculate the path of the blowing or suction outgoing characteristic before the discontinuation of blowing or suction, we must know how $\tau/\rho q^2$, τ/τ_w , $[(pv/\rho) + q^2v]/q^2$ and V/U_∞ vary with y/δ and blowing. Fortunately, there are τ/τ_w and V/U_∞ distributions given by Simpson [6] for his upstream suction data and for nearly the same blowing and Re_δ condition as the upstream Levitch data, so we can use these distributions. However, there is no known data des-

cribing in detail how the required turbulence quantities vary with blowing or suction. Levitch did not measure $\overline{w^2}/U_\infty^2$, nor attempt to describe how

$$\left(\frac{\overline{pv}}{\rho} + \frac{1}{2}\overline{q^2v}\right)/\overline{q^2}$$

changed with blowing. Hence we must make some plausibility argument as to how these quantities vary.

Plots of $\tau/\rho u^2$ from the blown and unblown data of Levitch and the unblown data of Klebanoff [4] appear to correlate on y/δ (Fig. 11). Likewise $\overline{u^2}/v^2$ correlates with y/δ for the blown and unblown data. Hence, it is a plausible assumption that blown and unblown $\overline{u^2}/w^2$ also correlate with y/δ . This means that $\tau/\rho q^2$ is a function of y/δ and is independent of blowing.

The assumptions concerning the turbulence energy diffusion velocity $V_p = [(\overline{pv}/\rho) + \frac{1}{2}\overline{q^2v}]/\overline{q^2/2}$ with blowing have less experimental support since no measurement of even $\overline{q^2v}$ with blowing was made by Levitch. However, on the rather skimpy evidence that other related quantities are independent of blowing and moderate suction, it appears that

$$V_p / \left(\frac{\tau_{\max}}{\rho_\infty U_\infty} \right)$$

is independent of blowing or moderate suction. First, the data of Simpson, Whitten and Moffat [10] showed that the turbulent Prandtl number distribution with y/δ was independent of blowing. It was also demonstrated with a rather crude model that with the turbulence energy diffusion velocity distribution independent of blowing but scaled on the entrainment velocity, one could calculate the turbulent Prandtl number distribution to be independent of blowing. Bradshaw [15] and Bradshaw, Ferriss and Atwell [4] have shown that the turbulence energy diffusion velocity at the outer edge of the boundary layer, or the entrainment velocity, is proportional to $\tau_{\max}/\rho_\infty U_\infty^2$ in the outer part of an unblown boundary layer:

$$\frac{V_{p\infty}}{U_\infty} = 10 \frac{\tau_{\max}}{\rho U_\infty^2}$$

Simpson [12] found that this equation applies for his blown layers with a slightly lower constant of 9. Furthermore, calculations performed by Bradshaw *et al.* of a blown boundary layer assuming

$$\left(V_p / \left(\frac{\tau_{\max}}{\rho U_\infty} \right) \right)$$

EFFET D'UNE DISCONTINUITÉ DANS LE SOUFFLAGE PARIÉTAL SUR LA COUCHE LIMITE TURBULENTE INCOMPRESSIBLE

Résumé—On rapporte des expériences sur les couches limites turbulentes bidimensionnelles de fluide incompressible pour lesquelles existe un changement brusque de soufflage pariétal. Les résultats sur le frottement à la paroi et le profil de vitesse moyenne indiquent que l'écoulement s'adapte asymptotiquement

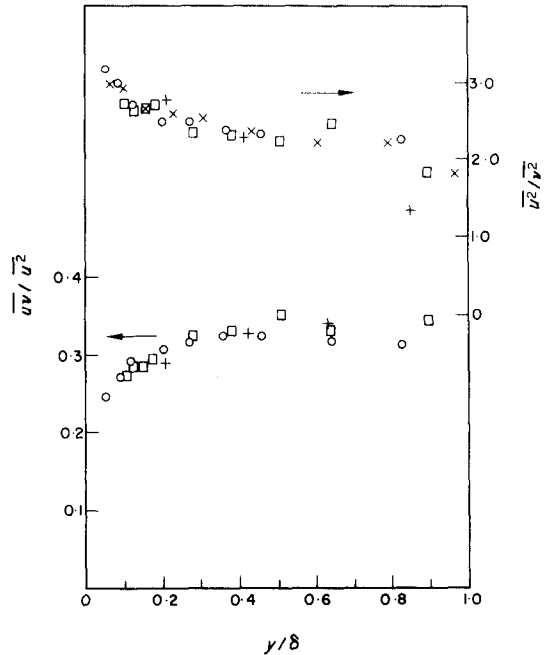


FIG. 11. Turbulence data of Levitch [3], $-\overline{uv}/u^2$ and $\overline{u^2}/v^2$ vs. y/δ .

V_w/U_∞	Re_θ	
x 0.00	3145	} Levitch
□ 0.0045	2915	
○ 0.0045	4060	
+ 0.00	7700	Klebanoff

independent of blowing were in good agreement with experimental results. Hence, it is a plausible assumption that the distribution of

$$\left(\frac{\overline{pv}}{\rho} + \frac{1}{2}\overline{q^2v}\right)/\overline{q^2} \left(\frac{\tau_{\max}}{\rho U_\infty}\right)$$

with y/δ remains unchanged with blowing.

vers l'aval au nombre de Reynolds relatif à l'épaisseur de quantité de mouvement et aux conditions de soufflage. On trouve qu'au cours de la longueur de relaxation, l'écoulement est séparé par une trajectoire à "point de pénétration" en une région extérieure décrite par les conditions d'amont et en une région intérieure qui dépend des conditions locales de soufflage. La forme de ces trajectoires paraît être très indépendante des conditions de paroi en aval.

On trouve que les trajectoires à point de pénétration coïncident étroitement avec la caractéristique tournée vers l'extérieur du système hyperbolique d'équations aux dérivées partielles présentée par Bradshaw, Ferris et Atwell [4]. Ces résultats suggèrent que la caractéristique externe est plus qu'un résultat mathématique et peut être observée expérimentalement avec des écoulements à changement brusque de soufflage pariétal.

DER EINFLUSS EINER DISKONTINUIERLICHEN WANDAUSBLASUNG AUF DIE TURBULENTE INKOMPRESSIBLE GRENZSCHICHT

Zusammenfassung—Es wird über Versuche an zweidimensionalen, inkompressiblen, turbulenten Grenzschichten mit plötzlicher Änderung der Wandausblasung berichtet. Die Ergebnisse für die Wandreibung und das mittlere Geschwindigkeitsprofil deuten an, dass sich die Strömung stromabwärts asymptotisch einem Verhalten nähert, wie es der mit der örtlichen Impulsverlustdicke gebildeten Reynolds-Zahl und den Ausblasebedingungen entspricht. Man findet, dass innerhalb der Ausgleichsstrecke eine "Durchdringungspunkt"-Linie die Strömung in ein äusseres Gebiet, das sich durch Bedingungen stromaufwärts beschreiben lässt, und ein inneres Gebiet aufteilt, das von den örtlichen Ausblasebedingungen abhängt. Die Lage dieser Linien scheint ziemlich unabhängig von den Wandbedingungen stromabwärts zu sein.

Die Durchdringungspunkt-Linien fallen fast mit der letzten stromaufwärts ausgehenden Charakteristik des Satzes der den Vorgang beschreibenden partiellen Differentialgleichungen hyperbolischen Typs zusammen, wie sie von Bradshaw, Ferris und Atwell [4] angegeben werden. Diese Ergebnisse zeigen, dass diese Charakteristik mehr als ein mathematisches Ergebnis ist und bei Strömungen mit plötzlichen Änderungen der Wandausblasung experimentell beobachtet werden können.

ВЛИЯНИЕ ВНЕЗАПНОГО ИЗМЕНЕНИЯ ОБДУВА СТЕНКИ НА ТУРБУЛЕНТНЫЙ ПОГРАНИЧНЫЙ СЛОЙ

Аннотация—Приводятся экспериментальные результаты по двумерным несжимаемым турбулентным пограничным слоям при резком изменении обдува стенки. Результаты измерений поверхностного трения и профиля средней скорости показывают, что ассимптотически вниз по потоку течение определяется локальным числом Рейнольдса, вычисленным по толщине потери импульса, и условиями вдува. Показано, что на длине релаксации поток разделяется траекторией «точки проникновения» на внешнюю область, описываемую условиями вверх по потоку, и внутреннюю область, зависящую от условий локального вдува. Оказывается, что путь этих траекторий почти не зависит от условия на стенке вниз по потоку.

Найдено, что траектории точки проникновения хорошо совпадают с последней, полученной вверх по потоку, характеристикой гиперболической системы основных дифференциальных уравнений в частных производных, представленных в работе [4]. Эти результаты предполагают, что полученная характеристика является более, чем математический результат, и может быть найдена экспериментально в потоках с резкими изменениями обдува стенки.